

Numerical and Experimental Analyses of Track Shoe Patterns for Vehicle on Sandy Terrain

Ignatius Pulung Nurprasetyo^{a,*}, Wirya Wicaksana^b, Siti Zulaikah^c, Bentang Arief Budiman^d

^aFaculty of Mechanical and Aerospace Engineering, Institut Teknologi Bandung. Email: ipn@ftmd.itb.ac.id

^bFaculty of Mechanical and Aerospace Engineering, Institut Teknologi Bandung. Email: wiryawicak@yahoo.com

^cNational Center for Sustainable Transportation Technology. Email: siti.zulaikah@my.sampoernauniversity.ac.id

^dFaculty of Mechanical and Aerospace Engineering, Institut Teknologi Bandung. Email: bentang@ftmd.itb.ac.id

Abstract

A track is a vehicle propulsion system that consists of a continuous band of chains connected with track shoes or may be entirely made of rubber. The track system is still commonly used on various vehicles, including bulldozers, excavators, tanks, and tractors, and has recently been used in lunar expedition vehicles. A tracked vehicle is mainly designed to provide better mobility in rough, uneven, or slippery terrain. The main component of the track system is track shoes or so-called grousers. This track shoe geometry will determine the tractive performance of the vehicle. If an incorrect shape is used, the excavator will most likely slip. The previous study approached this traction problem by using the semi-empirical method. However, until now, the track geometry and traction relation are still unclear. This research focuses on the effects of track shoe geometry on tractive performance and vehicle climbing ability. The analysis was mainly conducted with a DEM (Discrete Element Method) simulation. The result from the experimental test is also confirmed using a small-scale RC prototype on simulated terrain with different slope variations. It is proven that the grouser height directly affects the climbing performance of tracked vehicles. A higher grouser height proves to be better at a higher inclination slope. However, for a low inclination angle, the flattened track was better. The traction result from the EDEM simulation also yields a similar result. However, higher usable traction means more friction is generated; therefore, the track with higher traction also takes more energy to cover the same distance.

Keywords: Sandy terrain vehicle; track shoe; vehicle tractive performance

1. Introduction

Since the early 20th century, tracked vehicles have been developed for various off-road environments such as agriculture, construction, military, particular logistics, and even space exploration [1]–[3]. Tracks system can give excellent ground holding capability and mobility through very rough terrain better than wheels [3]–[6]. Wide tracks help distribute the vehicle's weight over a large area, decreasing the ground pressure, thus preventing it from sinking in sandy or soft ground [3]. The tractive performance of a tracked vehicle is influenced by how the track interacts with the soil, which strongly depends on the shape of the track, soil composition, and soil properties [7], [8].

There have been previous studies regarding the effect of track shape on tractive performance. For instance, Wang et al. examined the influence of grouser thickness and grouser height on traction by using a grouser shoe model [9]. They discovered that the optimal grouser height

depended on the composition of the soil and the moisture content of the soil. The complex terramechanics problem was complicated to be solved fully theoretically [10], [11]. Therefore, the prediction of vehicle traction on soft ground has been investigated using an empirical and semi-empirical method. Several research studies have demonstrated the reasonable accuracy of semi-empirical techniques in traction prediction [12]–[15]. The Bekker traction model equations use the relationship between specific physical soil characteristics and shearing strength to predict off-road vehicle mobility [15], [16]. Bekker considers wheels and tracks as simple loading surfaces with similar forms but different lengths and widths. The analogy was extrapolated between soil shear produced by laboratory crawlers to track vehicles and does not consider the grouser shape and vehicle driving parameters.

With the rapid development in computer technology and computational methods, people have come up with other methods that can be used, namely, the discrete element method (DEM) [15], [17]. DEM simulation uses a multi-particle simulation that treats each particle individually [18]. Particle parameters such as shape, size, density, Young's Modulus, Poisson's ratio, coefficient of restitution, and friction coefficient can be easily specified

*Corresponding author.

Jl. Ganesa No.10, Lb. Siliwangi, Coblong
Bandung, Jawa Barat, Indonesia
40132

to model a real-life problem. Recently, these methods have become more widely used in addressing soil-body contact problems [19], [20].

The main objectives of this research are to investigate the track shoe and soil interaction and determine how different track shoe geometry may affect the vehicle's performance, mainly the climbing ability as well as the traction of the vehicle, and to determine the optimum grouser height for a tracked vehicle on sandy terrain at various inclination slopes.

This research is expected to provide a better understanding of track vehicles, specifically track shoes, and how various parameters will affect the overall vehicle performance. The results from the experiment could serve as a reference for future EDEM experiments and help engineers in developing new track shoes for the future, as well as mechanics or users who are looking for a new track shoe.

2. Methodology

2.1. Discrete Element Method

Given that sand is composed of many small particles, this research was approached using computational analysis, which is EDEM software. The forces acting upon one piece of the track shoe and their interaction with the particles would be found. Beforehand, the geometry model was constructed using SolidWorks. Figure 1 shows the EDEM system, including sand particles, a piece of track shoe, and a box. The gravitational force is in the z-direction, and the weight of the track shoe was assumed to be the weight of the small-scale RC excavator. It is 16 N divided by the total number of track shoes in direct contact with the sand, which is 42 tracks.

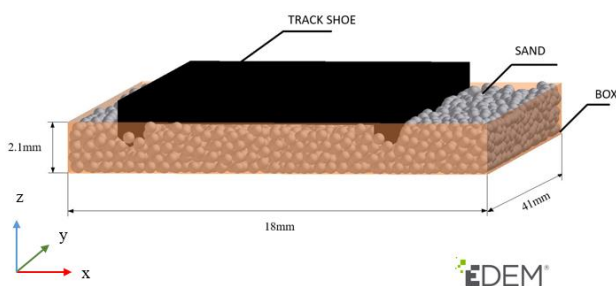


Figure 1. EDEM simulation

Table 1. Sand properties

Bulk Material Properties	Magnitude	Unit
Poisson's Ratio	0.25	-
Solid Density	1460	kg/m ³
Shear Modulus	69000000	Pa
Coefficient of Restitution	0.64	-
Coefficient of Static Friction	0.6	-
Coefficient of Rolling Friction	0.4	-
Particle Diameter	0.2604	mm
Total Particle	9000	particle

EDEM software has several particle shape libraries, including sphere, dual sphere, triple sphere, and tetrahedral. None of these could represent the shape of the real sand that is not uniform. Thus, the sand was depicted with a spherical particle as the simplest and fastest approach for this simulation. After choosing the shape, several particle parameters must be inputted into the program. Due to sand properties varying depending on its composition, some of the properties listed in Table 1 were assumed to be well-graded sand except for the particle diameter and density measured directly.

Figure 2a shows how the grain size of sand can be approximated by using a simple digital microscope with 50 times magnification. The sand is highlighted with a black line. Before starting the experiment, the pixel size of 1 mm was measured for the reference point and calculated to be 394 pixels. By the effective diameter method, the average sand grain size was calculated to be 102.6 pixels and then converted to mm, generating a grain size of 0.2604 mm. Figure 2b shows the outer and inner diameters approaching the sand diameter.

The discrete element method principle portrays the soil (terrain) as an assemblage of several discrete elements. Sand has almost no cohesion when water is not present; thus, dry sand using the discrete element method can be approached. Figure 2c depicts one circular element in the EDEM plane.

EDEM allows analyzing the track and sand interaction by examining the mechanical interactions between the track and adjacent elements and those between the contacting elements. Elements in contact with the track surface receive contact forces from the track. Elements not in contact with the track surface receive contact forces from other contacting elements. The magnitudes of the contact forces are assumed to be related to the relative displacement and relative velocity of the contacting elements, dependent upon the model for the mechanical property of the elements used.

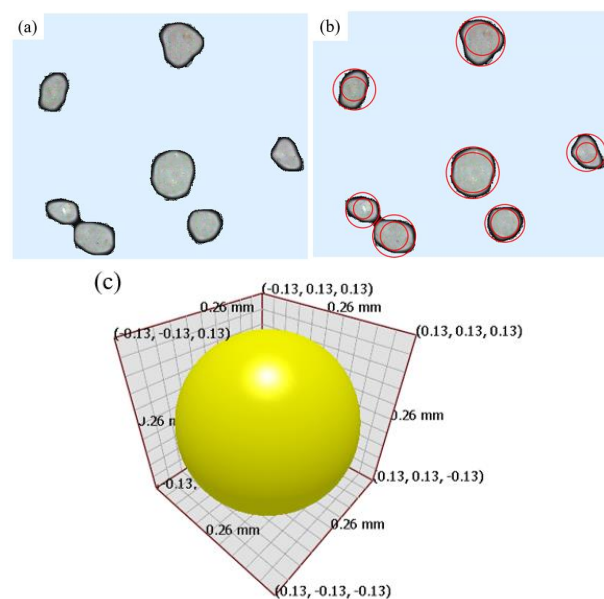


Figure 2. (a) Captured grains of sand under microscope; (b) Inner and outer diameter measurement under microscope; (c) Representative ball model for grains of sand in DEM

2.2. Experimental Method

The experiment setup mainly included a 1:14 scale RC excavator, digital weight scale, spirit level, digital Avometer, sand, video camera, leveler, measuring tape, tripod, and plywood. The experiment was conducted by running a small-scale RC excavator on well-graded sand. Beforehand, three different track setups were created by modifying the grouser height to simulate the three different grouser geometries. The track was produced by modifying the standard track using resin casting. For each setup, the performance would be compared to which one is the best in terms of traction and climbing ability.

Due to equipment and tool limitations, only three tracks were used in this experiment (Fig. 3). The first setup was the standard track obtained from the manufacturer without any modification, which used plastic material with clear concave and convex surfaces in their track shoes. The second setup was created to simulate low grouser height. This grouser has the space in between that is filled with resin, generating flatter and smoother surfaces. Lastly, the third setup was created to simulate high grouser height. A small stick of wood as wide as the track size was fixed to the track's surface using resin as its adhesive, generating a higher grouser height but still maintaining the stiffness.

For all three tracks, the weight was measured using a digital scale. As a result, setup 1 has the lightest weight at only 38 grams each; setup 2 has a weight of 41 grams each; and setup 3 has the heaviest weight at 53 grams each. Even though this weight difference is slight, it is predicted to still affect the RC excavator's performance.

All three setups were tested with the excavator on a sandy surface inside a plywood box. This box is custom-made and has dimensions 110 cm long, 40 cm wide, and 7.5 cm in height. Even though the sand only fills up to 75% of the box's maximum capacity or around 5 cm. Afterward, on the sides of the box, a measuring tape is attached to help monitor the distance traveled by the excavator. Figure 4a shows the main experiment apparatus used in this research.

For better accuracy, the sand was leveled, and the bumpiness was tested with a spirit level for each run to ensure no bumps or holes on the sand. The test was initially performed with slopes of 10°, 20°, and 30°. However, the excavator always failed or became stuck at the 30° slopes, as shown in Fig. 4b. As a result, the increment was changed to 5°. The excavator is run through uphill and downhill set configurations with 0°, 13°, 18°, and 23° slopes for each setup. All data is captured with the video camera.

All the grouser parameters of this work were defined as follows. The model used W of 16 N, L of 1 cm, h of 0.1, 0.3, and 0.5 cm, t of 0.2 cm, b of 4 cm, and λ of 0.1. The grouser length, vertical load, thickness, width, and thickness ratio are fixed due to limitations in manufacturing. In other words, this work focuses more on the effect of grouser height. Since the excavator motor speed cannot be precisely adjusted and only depend on the battery condition. Hence, the battery voltage was monitored for every run to ensure the speed was not affected by the battery.



Figure 3. Three different track setups: (a) Setup 1; (b) Setup 2; (c) Setup 3

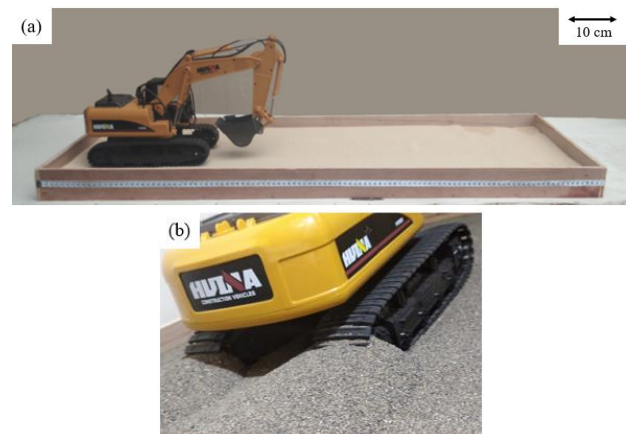


Figure 4. (a) Experimental apparatus; (b) Example of sinking excavator

3. Result and Discussion

3.1. Climbing Ability

Overall, three different setups (track profiles) were tested in this research. A video camera was used and placed on the side of the apparatus using a fixed tripod. This video camera can take videos with a resolution of 1080p at 24 FPS (frames per second). Afterward, the video would be processed in video editing software. The video editing software used is Adobe Premiere due to its user interface ease and its capability to process various video formats. Subsequently, the unnecessary frame is removed in this software, leaving only the part when the excavator starts moving until the excavator touches the other side of the box. Therefore, the timecode for every run can be obtained. Timecode values are a way of numbering frames in the video. Standardized by SMPTE (Society of Motion Picture and Television Engineers), video timecode is usually represented as an hour, minute, second; then, each

frame number is separated by a colon (:). The timecode is then converted to seconds by dividing the frames by 24. Since the distance traveled by the excavator, the speed in cm/s can be obtained.

Figure 5 is the bar graph obtained from the experimental results. In this graph, the speed for every setup and every inclination angle can be observed. The graph shows that the speed difference is relatively small (<5 cm/s). In addition to speed data, how steep the excavator’s ability to climb also can be found by investigating the angle of failure or the angle at which the excavator cannot climb anymore. The failure angles for setups 1, 2, and 3 are 25.93°, 24.87°, and 28.20°, respectively. It can be seen that for track shoe of setup 2, the speed difference of downhill and uphill is highest than other setups. This can occur because the setup 2 does not have sufficient grip to avoid slip between the track shoe and sand.

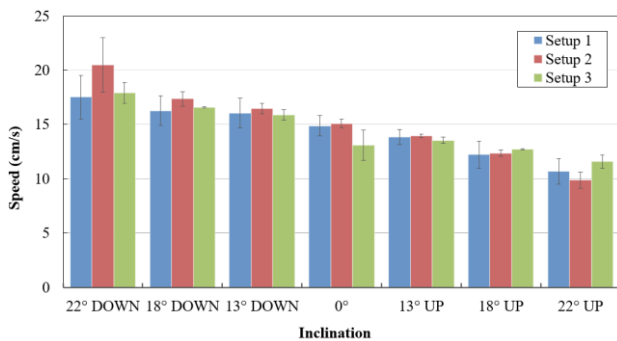


Figure 5. Speed graph

3.2. Slip ratio

The slip ratio is a non-dimensional value calculated from the motor revolution and actual distance traveled. By the slip ratio equation for a tracked vehicle, the slip ratio for each setup is found. The slip ratio value lies between zero (no slippage) and one (total slippage). In this research, the slip ratio was calculated using speed at the steepest inclination (22°), and the RPM was calculated from the total wheel rotation per minute. Table 2 is the result of the slip ratio.

The slip ratio for downhill is negative because the excavator travels faster than the wheel rotation itself. Since the slip ratios are not zero, the excavator experiences slip phenomena.

Table 2. Slip ratio

	Setup 1	Setup 2	Setup 3
r (cm)	2.4	2.4	2.4
h (cm)	0.3	0.1	0.5
RPM	55	55	55
ω (rad/s)	5.76	5.76	5.76
Speed uphill (cm/s)	12.05	10.73	12.28
Speed downhill (cm/s)	19.85	22	18.99
Slip ratio uphill	0.225	0.255	0.265
Slip ratio downhill	-0.276	-0.528	-0.137

3.3. EDEM Results

There are three main phases in the EDEM experiment. The first phase was the particle generation phase; the total number of particles was set at 9000 particles. The second phase was the moving phase. The track shoe started moving with a starting velocity of 0.09 m/s and 0 m/s² acceleration. Finally, the settling phase was where the track stopped moving and the particles settled. The total time from start to finish was 0.14 s. Afterward, the force in the x-direction is plotted on a graph. Since the excavator is supported by 42 track shoes when stationary, the forces for one shoe are multiplied by 42 to estimate the traction produced. The model of track shoes is made as close as possible to make the result comparable to the experiment conducted prior.

Figure 6a depicts setup 1 of track shoe and sands particles in the EDEM plane. Figure 6b depicts the sand compressive force contour from the isometric view. Figure 6c depicts the sand compressive force contour from the top view.

Figure 7a depicts setup 2 of track shoe and sands particle in the EDEM plane. Figure 7b depicts the sand compressive force contour from the isometric view. Figure 7c depicts the sand compressive force contour from the top view.

Figure 8a depicts setup 3 of track shoe and sands particle in the EDEM plane. Figure 8b depicts the sand compressive force contour from the isometric view. Figure 8c depicts the sand compressive force contour from the top view.

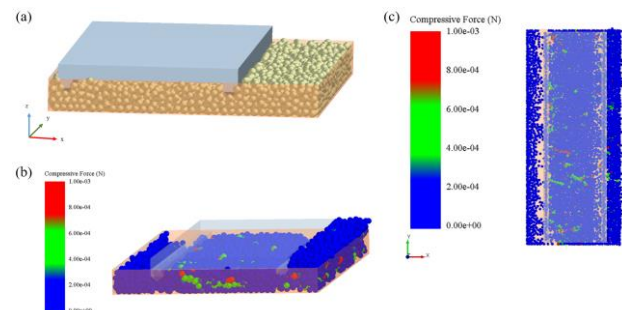


Figure 6. (a) EDEM setup 1; (b) Compressive force of EDEM setup 1; (c) Pressure contour of setup 1

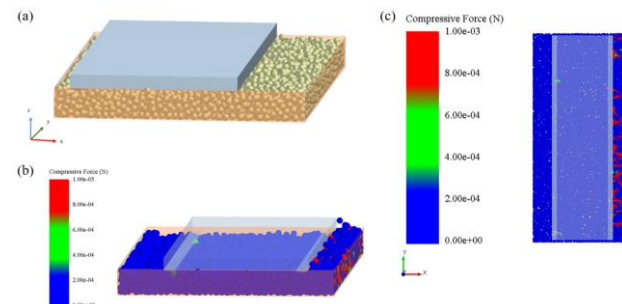


Figure 7. (a) EDEM setup 2; (b) Compressive force of EDEM setup 2; (c) Pressure contour of setup 2

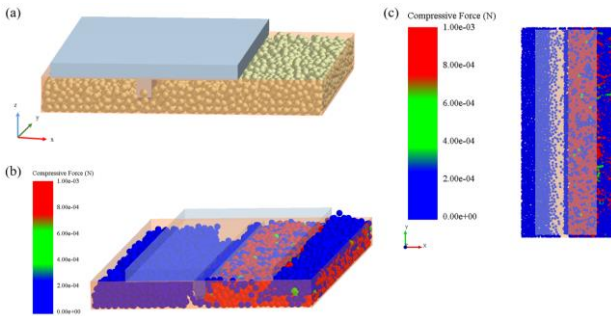


Figure 8. (a) EDEM setup 3; (b) Compressive force of EDEM setup 3; (c) Pressure contour of setup 3

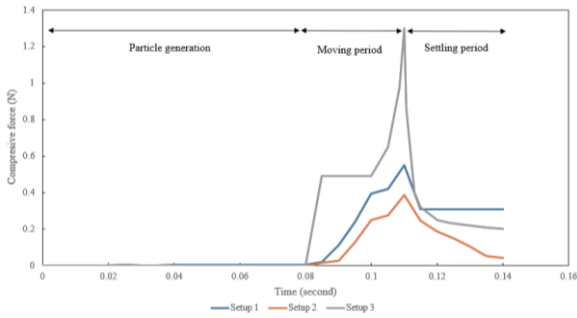


Figure 9. Plot of compressive force

The plot of Fig. 9 is the result of all EDEM. The x-axis represents time in second, and the y-axis represents the compressive force in Newton.

According to Fig. 9, the maximum force of setups 1, 2, and 3 are 0.549 N, 0.388 N, and 1.30 N, respectively. Then, by multiplying each of those results by 42, the final forces of setups 1, 2, and 3 are 23.1 N, 16.29 N, and 54.6 N, respectively. The whole set of the results is listed in Table 3, showing that setup 3 produced the highest traction force. Some errors probably occurred when it was compared to the actual traction.

3.4. Work Calculation

The excavator is assumed to move uphill with force equal to the total traction force obtained from the EDEM simulation. Then, the required work for each setup could be found if the excavator climbed the same 110 cm-long hills. To find the work, the formula is:

$$W = F \times s \tag{1}$$

Where W is work, F is force, and s is the distance traveled. Based on Fig. 10, the resultant force is traction force subtracted by $w \sin \theta$, and the distance is the sandbox length.

Table 3. Traction result

Setup	Max. compressive force (N)	Total traction (N)	Change (%)
1	0.55	23.1	Baseline
2	0.388	16.29	-29.48
3	1.3	54.6	136.36

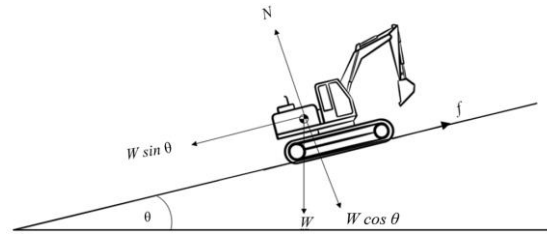


Figure 10. FBD of excavator

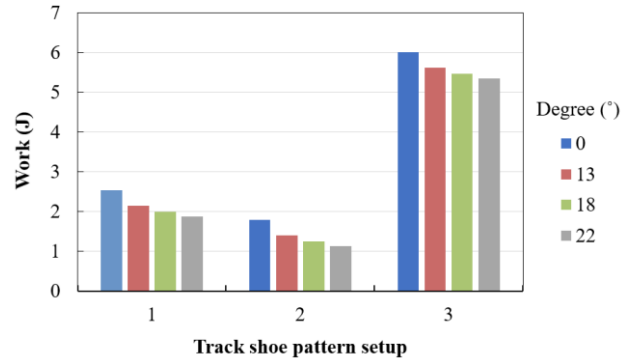


Figure 11. Work excavator

This data from the work calculation for each inclination is then plotted in Fig. 11. This graph can provide a general idea about the work for each track configuration. Although this data does not represent the actual work performed by the excavator, it is expected that the result will be as close as possible. Moreover, assuming no slip occurs, the maximum work done by the excavator can be obtained and given to propel the excavator forward.

3.5. Sand Pattern

The photos of the sand pattern for every run have been taken as a comparison. As shown in Fig. 12, there was a variety of different patterns. The track with no trailing lines on the sides indicates that the track is not slipping, as depicted in Fig. 12a. Additionally, the pattern with no-slip occurred also showed that the track pattern is very clear and does not overlap with the adjacent track shoe. On the other hand, as depicted in Fig. 12b, lines formed on the sides of the track, indicating that slipping has occurred. From the setup configuration, setup 3 leaves a deeper penetration compared to two other setups; meanwhile, setup 2 slipping lines are more obvious compared to two other setups.

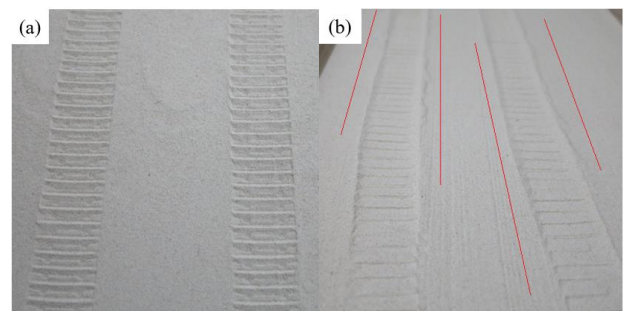


Figure 12. (a) Track pattern without slipping occurred; (b) Track pattern with slipping occurred

4. Conclusion

This research study has performed the simulation and experiment of track shoes on sandy terrain. The result shows that changing the grouser geometry, especially the grouser height, helps the excavator climb faster at a higher inclination slope greater than 18 degrees, while the lower inclination slope of fewer than 18 degrees does not contribute much or even slows the speed down slightly. A higher grouser height also demonstrates a greater climbing ability with the steeper hill of 28 degrees compared to 25 degrees from the standard track and 24 degrees from the flat track. EDEM simulation yields a similar result for a higher grouser height (setup 3) has 136% better traction force than the standard track (setup 1), meaning that setup 3, assuming no slippage, requires more energy to cover the same distance. Therefore, the tracked vehicle operated on sandy terrain with a steep slope would perform better when applying higher grouser height; meanwhile, applying flat or lower grouser height is suggested only when a tracked vehicle operated in flat terrain.

References

- [1] G. Ferretti and R. Girelli, "Modelling and simulation of an agricultural tracked vehicle," *J. Terramechanics*, vol. 36, no. 3, pp. 139–158, 1999.
- [2] Z. Hryciów and P. Rybak, "Numerical research of the high-speed military vehicle track," in *AIP Conference Proceedings*, 2019, vol. 2078, no. 1, p. 020029.
- [3] J. T. Cook, L. E. Ray, and J. H. Lever, "Mobility Enhancement of Heavy-Duty Tracked Vehicles Under Load Using Real-Time Terrain Characterization, Traction Control, and a Towing Winch," *J. Dyn. Syst. Meas. Control*, vol. 141, no. 7, 2019.
- [4] S. A. Shaikh et al., "Effect of grouser height on the tractive performance of single grouser shoe under different soil moisture contents in clay loam terrain," *Sustainability*, vol. 13, no. 3, p. 1156, 2021.
- [5] T. Nabaglo, J. Kowal, and A. Jurkiewicz, "Construction of a parametrized tracked vehicle model and its simulation in MSC.ADAMS program," *J. Low Freq. Noise, Vib. Act. Control*, vol. 32, no. 1–2, pp. 167–173, 2013.
- [6] Y. Yang, T. Cai, and X. Xu, "Track Design of Track-Wheel Transport Vehicle and Strength Analysis of Important Components," in *InIOP Conference Series: Materials Science and Engineering 2020*, 2020, vol. 782, no. 2, p. 022058.
- [7] Z. Ding, Y. Li, and Z. Tang, "Theoretical Model for Prediction of Turning Resistance of Tracked Vehicle on Soft Terrain," *Math. Probl. Eng.*, vol. 2020, 2020.
- [8] M. J. Dwyer, "The tractive performance of wheeled vehicles," *J. Terramechanics*, vol. 21, no. 1, pp. 19–34, 1984.
- [9] X. L. Wang, N. Ito, K. Kito, K. Sato, and M. Yamashita, "Studies on Grouser Shoe Dimension for Optimum Tractive Performance (Part 3) Comparison of predictive and experimental traction of track's grouser," *J. Japanese Soc. Agric. Mach.*, vol. 65, no. 5, pp. 64–69, 2003.
- [10] E. Leflaive, "Mechanics of wheels on soft soils—A method for presenting test results," *J. Terramechanics*, vol. 3, no. 1, pp. 13–22, 1966.
- [11] S. Taheri, C. Sandu, S. Taheri, E. Pinto, and D. Gorsich, "A technical survey on Terramechanics models for tire-terrain interaction used in modeling and simulation of wheeled vehicles," *J. Terramechanics*, vol. 57, pp. 1–22, 2015.
- [12] D. Gee-Clough, M. McAllister, G. Pearson, and D. W. Evernden, "The empirical prediction of tractor-implement field performance," *J. terramechanics*, vol. 15, no. 2, pp. 81–94, 1978.
- [13] M. G. Bekker, *Introduction to terrain-vehicle systems, part i: The terrain, part ii: The vehicle*. Michigan Univ Ann Arbor, 1969.
- [14] J. Y. Wong, *Terramechanics and off-road vehicle engineering: terrain behaviour, off-road vehicle performance and design*. Butterworth-heinemann, 2009.
- [15] A. Nicolini, F. Mocera, and A. Soma, "Multibody simulation of a tracked vehicle with deformable ground contact model," *Proc. Inst. Mech. Eng. Part K J. Multi-body Dyn.*, vol. 233, no. 1, pp. 152–162, 2019.
- [16] G. R. Gerhart, "The bekker model analysis for small robotic vehicles," *SAE Trans.*, pp. 317–324, 2004.
- [17] F. Mocera, A. Somà, and A. Nicolini, "Grousers Effect in Tracked Vehicle Multibody Dynamics with Deformable Terrain Contact Model," *Appl. Sci.*, vol. 10, no. 18, p. 6581, 2020.
- [18] S. Wangchai, "Numerical simulation of the flow of agricultural seeds inside a rotary drum dryer by DEM," in *IOP Conference Series: Earth and Environmental Science*, 2019, vol. 301, no. 1, p. 012048.
- [19] A. A. Tagar et al., "Finite element simulation of soil failure patterns under soil bin and field testing conditions," *Soil Tillage Res.*, vol. 145, pp. 157–170, 2015.
- [20] A. Yokoyama, H. Nakashima, H. Shimizu, J. Miyasaka, and K. Ohdoi, "Effect of open spaces between grousers on the gross traction of a track shoe for lightweight vehicles analyzed using 2D DEM," *J. Terramechanics*, vol. 90, pp. 31–40, 2020.